CMLS, Cell. Mol. Life Sci. 60 (2003) 1489–1503
1420-682X/03/071489-15
DOI 10.1007/s00018-003-3150-4

CMLS Cellular and Molecular Life Sciences

Research Article

β-phenylethyl isothiocyanate-mediated apoptosis in hepatoma HepG2 cells

P. Rose[a,*], M. Whiteman[b], S. H. Huang[b], B. Halliwell[b] and C. N. Ong[a]

[a] Department of Community, Occupational and Family Medicine, MD3, National University of Singapore, 16 Medical Drive, 117597 Singapore, Fax: 65 779 1489, e-mail: cofpcr@nus.edu.sg
[b] Antioxidant and Oxidant Research Group, Department of Biochemistry, National University of Singapore, 8 Medical Drive, 117597 Singapore

Received 23 December 2002; accepted 22 April 2003

Abstract. β-Phenylethyl isothiocyanate (PEITC) is a promising chemoprotective compound that is routinely consumed in the diet as its glucosinolate precursor. Previous studies have shown that PEITC can inhibit phase I enzymes and induce phase II detoxification enzymes along with apoptosis in vitro. The detailed mechanisms involved in the apoptotic cascade, however, have not been elucidated. In the present study, we demonstrate that PEITC can induce apoptosis in hepatoma HepG2 cells in a concentration- and time-dependant manner as determined by TUNEL positive and SubG1 population analysis. Caspase-3-like activity and poly(ADP-ribosyl)polymerase cleavage increased during treatment with 20 μM PEITC; high concentrations, however, induced necrosis. Pre-treatment with Z-VAD-FMK and the caspase-3-specific inhibitor Ac-DEVD-CHO prevented PEITC-induced apoptosis, as determined by caspase-3-like activity and DNA fragmentation. Additional investigations also showed that at concentrations of 5–10 μM PEITC, DNA synthesis was inhibited and G2/M phase cell cycle arrest occurred, correlating with an alteration in cyclin B1 and $p34^{cdc2}$ protein levels. Furthermore, we also demonstrate a concentration- and time-dependant burst of superoxide ($O_2^{\bullet -}$) in PEITC-treated cells. However, pre- and co-treatment with the free radical scavengers Trolox, ascorbate, mannitol, uric acid and the superoxide mimetic manganese (III) tetrakis (N-methyl-2-pyridyl) porphyrin failed to prevent PEITC-mediated apoptosis. Taken together, these results suggest that PEITC potently induces apoptosis and cell cycle arrest in HepG2 cells and that the generation of reactive oxygen species appears to be a secondary effect.

Key words. Apoptosis; cell cycle arrest; β-phenylethyl isothiocyanate; oxidative stress.

Epidemiological evidence suggests that high consumption of fruits and vegetables can prevent the development of a wide range of cancers such as colon, lung and oesophageal [1, 2]. The reduction especially in the gastrointestinal tract is associated with a high intake of green leaf vegetables such as those found in the Brassicaceae [1]. The chemoprotective effects are believed to be due in part to a group of phytochemicals known as glucosinolates (GSLs) that under the action of myrosinase (thioglucoside glucohydrolase, EC 3.2.3.1) are converted to the bioactive isothiocyanates (ITCs), following tissue disruption and or hydrolysis by enteric gut bacteria [3, 4].
Mechanistic studies indicate that ITCs, especially the ω-methylsulphinylalkyl (Msalk) ITCs, are potent phase II enzyme inducers up-regulating gene expression and enzyme activity in a variety of tissues. Glutathione-S-transferases (GSTs) (EC 2.5.1.18), quinone reductase (QR) [NAD(P)H: (quinone acceptor) oxidoreductase, EC 1.6.99.2] and UDP-glucuronosyl transferases (EC

* Corresponding author.

2.4.1.17) have all been observed to increase in vivo and in vitro when exposed to ITCs [5–7]. The induction of phase II detoxification enzymes is believed to give these compounds their chemoprotective attributes. Indeed, consumption of watercress has been shown to alter the metabolism of the tobacco-specific carcinogen 4-(methylnitrosamino)-1-(3-pyridyl)-1-butanone (NNK) in humans by the proposed stimulation of UDP-glucuronosyl transferases [8]. Epidemiological studies complement the above finding by showing a strong correlation between exposure to dietary-derived ITCs and a reduced risk of lung cancer [9, 10]. Moreover, a high intake of broccoli *Brassica oleracea* var. *italica,* a species known to contain sulphoraphane (MSB), has also been associated with a reduced risk of colon cancer [11].

More recent studies have also begun to explore the possible role of ITCs in the induction of apoptosis in mammalian cells. Reports have demonstrated the ability of MSB, a major ITC found in broccoli to inhibit cell proliferation by inducing the expression of cyclins A and B1 and apoptosis in colonic HT29 cells [12]. Cell cycle arrest and apoptosis induced by MSB and its N-acetylcysteine mercapturic acid metabolite S-(N-methylsulphinylbutyl)-L-N-acetylcysteine in human prostate cancer cells has also been described [13].

Watercress [*Rorripa nasturtium aquaticum* (L.) Hayek, syn. *Nasturtium officinale* R. Br] is an exceptionally rich source of β-phenylethyl isothiocyanate (PEITC) in the form of its GSL precursor. In addition to its ability to induce phase II detoxification enzymes and inhibit phase I enzymes, PEITC can also induce apoptosis. Evidence suggests that both p53-dependent and -independent mechanisms are involved [14–16]. Inhibition of cell proliferation, caspase-3 and -8 activation and bid cleavage have been described for PEITC-induced apoptosis in HL60 cells. Furthermore, the mercapturic acid metabolites derived from the conjugation of PEITC with N-acetylcysteine and cysteine are also potent apoptotic agents both in vivo and in vitro [17–19].

In the present study we investigated the ability of PEITC to induce apoptosis and cell cycle arrest using hepatoma HepG2 cells as a hepatic model, and determined whether reactive oxygen species (ROS) had any involvement in this cascade. PEITC induced typical morphological changes associated with the induction of apoptosis such as cell shrinkage, nuclear condensation and membrane blebbing. Time- and concentration-dependent increases in lactate dehydrogenase (LDH) leakage, caspase-3 like activity, poly(ADP-ribosyl)polymerase (PARP) cleavage and DNA fragmentation were observed. We also demonstrate that PEITC-induced G2/M phase arrest correlates with a committed increase in cyclin B1 and a decrease in $p34^{cdc2}$ protein levels. In addition, one of the major questions that still remains to be elucidated in the mechanisms of ITC-induced apoptosis is the signalling event that leads to the subsequent activation of the apoptotic cascade. The role of ROS generation has been well-characterised for several apoptotic agents such as UV-B, tumour necrosis factor-α (TNF-α), vincristine and vanadate and is suggested to contribute to the signalling events leading to programmed cell death [20–23]. Recent reports have also suggested a possible role for ROS in benzyl isothiocyanate-mediated apoptosis [24]. In our study, we observed an early generation of superoxide; co- and pretreatment with several antioxidants, however, failed to prevent PEITC-mediated apoptosis.

Materials and methods

Cells and reagents

Chemicals were of the highest quality available. The human hepatoma HepG2 cell line was purchased from the American Type Culture Collection (Rockville, Md.). PEITC, dimethyl sulphoxide (DMSO), RNase A, paraformaldehyde, sodium dodecylsulphate (SDS), penicillin and streptomycin were purchased from Sigma-Aldrich (Poole, U. K.). Manganese(III)tetrakis (N-methyl-2-py-ridyl) porphyrin (MnPyP) was purchased from Calbio-chem (San Diego, Calif.). $^{15}N_2$ and ^{13}C heavy isotopic DNA base standards FAPy guanine, 8-OH guanine, 8-OH adenine, FAPy adenine, thymine glycol, 5,6-dihydroxyuracil, 5-(hydroxymethyl)uracil and 5-hydroxycytosine were purchased from Cambridge Isotope (Cambridge, Mass.). The remaining DNA bases were quantified using azathymine for the remaining pyrimidines, and 2,6-diaminopurine was used for the remaining purines as previously described [25]. CelluSep dialysis membranes with a relative molecular mass cut-off of 3500, silylation grade acetonitrile and bis(trimethylsilyl)trifluoracetamide (BSTFA) (containing 1% trimethylchlorosilane, TMCS) were obtained from Pierce (Rockford, Ill.). Distilled water passed through a purification system (Elga, High Wycombe, U. K.) was used for all purposes. Minimal essential medium (MEM), trypsin and fetal bovine serum (FBS) were purchased form GIBCO BRL (Gaithersburg, Md.). Propidium iodide (PI), dihydroethidium (DHE) and carboxy-2′,7′-dichlorofluorescein (carboxy-DCFDA) were purchased from Molecular Probes (Eugene, Ore.). The TUNEL assay kit and BrdU incorporation kit were from Roche Diagnostics (Mannheim, Germany).

Cell culture

HepG2 cells were cultured as described elsewhere [26]. In brief, HepG2 cells were cultured in complete MEM (containing 10% FBS, 100 U/ml penicillin, 100 mg/ml streptomycin, pH 7.4) in 75-cm^2 culture flasks at 37 °C in 5% CO_2 unless otherwise stated. After reaching 70–80% confluence, the complete MEM was removed and cells

were washed 2 × 1% in phosphate-buffered saline (PBS). Fresh MEM media, FBS free, was then added for the designated treatments. PEITC was dissolved in DMSO to a final concentration of 10 mM and diluted in media to the desired concentration such that the DMSO concentration was less than 0.1%.

Cell viability testing

Cell viability was determined by the MTT or the crystal violet assay as previously described [7, 27]. In brief, HepG2 cells were seeded at a density of 1×10^4 cells/well in a 96-well microtitre plate and incubated for 24 h. Following cell adhesion, the medium was replaced with MEM (FBS free) containing the designated concentrations of PEITC. Viability was measured by the colourimetric change using a plate reader at 595 nm for the MTT assay or 610 nm for crystal violet (model 3550; Bio-Rad, Hercules, Calif.).

Activity of LDH in the medium was measured using an Abbott VP Biochemical Analyser with the test kit (Abbott Laboratories, Irving, Tex.). The total LDH activity was determined by ultrasonication and assessed by expressing as percentage LDH leakage (LDH in medium/total LDH activity × 100).

TUNEL and BrdU incorporation assays

DNA fragmentation and BrdU incorporation in HepG2 cells was measured using the TdT-mediated dUTP nick end-labelling (TUNEL) and BrdU incorporation assay. The experiments were conducted following the manufacturer's instructions. From each treatment 10,000 cells were analysed using flow cytometry to determine the number of TUNEL positive cells (Coulter Epics Elite ESP, Miami, Fla.). Data were analysed using WinMDI 2.7 software (Scripps Institute, La Jolla, Calif.).

Sub-G1 analysis

Following the designated treatments, cells were scraped, washed 2 × 1% PBS, fixed and permeabilised with 70% ice-cold ethanol and incubated at 4 °C/2 h. Cells were then incubated for 30 min/37 °C in freshly prepared PI solution (0.1% Triton X-100, 200 µg/ml RNase A, and 20 µg/ml PI in PBS) followed by flow cytometry. Cell cycle changes were analysed by flow cytometry of at least 10,000 cells per sample. Data were analysed using WinMDI 2.7 software (Scripps Institute, La Jolla, Calif.) and the percentage of sub-G1 cells determined from histogram analysis as previously described [26].

Determination of cellular caspase-3-like activity

Caspase-3-like acitivity was determined spectrofluorometrically using the synthetic substrates Ac-DEVD-AFC (Bio-Rad). Briefly, cells were collected from each treatment by scraping and lysed on ice in cell lysis buffer (10 mM Tris-HCl, pH 7.5, 10 mM NaH_2PO_4, 130 mM NaCl, 1% Triton X-100 and 10 mM NaPPi) for 30 min. Cell homogenates were then incubated with synthetic substrate at 37 °C/2 h. The fluorescence intensity of the liberated AFC from the substrate was monitored using a spectrofluorometer (LS-5B; Perkin Elmer, Beaconsfield, UK) with an excitation wavelength of 390 nm and an emission wavelength of 510 nm.

Western blot analysis: PARP, cyclin B1 and $p34^{cdc2}$

Western blot analysis was used to determine changes in key apoptotic proteins. In brief, 20–30 µg of protein was subjected to a 7.5–10% SDS gel. Following electrophoresis, the protein was transferred to a nitrocellulose membrane at 4 °C and subsequently hybridized with either purified mouse anti-human PARP (clone AC10-5), cyclin B1 and $p34^{cdc2}$ (Santa Cruz Biotech, Santa Cruz, Calif.) or β-actin (Sigma-Aldrich, Poole, U. K.) and incubated with goat anti-mouse or rabbit IgG-horseradish peroxidase. Blots were visualised using the enhanced chemiluminescence ECL-plus Western blotting detection system (Amersham Biosciences, U. K.).

Measurement of intracellular superoxide and peroxide generation

Superoxide and peroxide generation were determined using the fluorescent probes DHE (excitation 488 nm, emission 620 nm) and carboxy-DCFDA (excitation 485 nm, emission 530 nm) using flow cytometry as previously described [28, 29]. In brief, at the end of designated treatments, cells were collected, washed twice with PBS and co-incubated with the recommended concentrations of DHE or carboxy-DCFDA (2.5 µM) in PBS for 15 min/37 °C. A minimum of 10,000 cells were analysed per treatment using flow cytometry. Data were analysed using WinMDI 2.7 software.

Analysis of DNA base modification by gas chromatography-mass spectrometry

Preparation, hydrolysis, derivatisation and analysis of samples were essentially performed as described previously [30–32]. Aliquots of 100 µg isolated DNA including 0.5 nmol of ^{15}N and ^{13}C heavy isotopes were freeze-dried under reduced pressure after addition of internal standards. Samples and commercial standards were subsequently hydrolysed by addition of 0.5 ml of 60% (v/v) formic acid and heating at 150 °C for 45 min in evacuated glass hydrolysis tubes. Samples were cooled, lyophilised and finally derivatised under a nitrogen atmosphere in poly(tetrafluoroethylene)-capped hypovials (Pierce) by adding 100 µl of a BSTFA [+ 1% TMCS/acetonitrile/ethanethiol (16:3:1 v/v] mixture. Samples were derivatised at room temperature for 2 h and then analysed by gas chromatography-mass spectrometry (GC-MS) (Hewlett-Packard, 6890II gas chromatography interfaced

with a Hewlett-Packard 5973A mass selective detector), as described elsewhere [30–32].

Statistical analysis

Histograms, dot plot, density plot and Western blot data are representative of at least three separate independent experiments conducted on separate days using freshly prepared reagents. All experimental data consists of the mean ± SE and were analysed by one-way ANOVA.

Results

Effects of PEITC on cell viability

The concentration-dependant changes in cell viability in PEITC-treated HepG2 cells were determined by the MTT assay as shown in figure 1. PEITC induced a concentration-dependant decrease in cell viability that was significant from the control as determined at 24 h (ANOVA, $p < 0.01$).

PEITC induced apoptosis in HepG2 cells

In the current study, apoptosis was evaluated using the TUNEL assay, LDH leakage, measurement of sub-G1 cells and changes in cell size and morphology. Time- and concentration-dependant increases in TUNEL-positive cells after treatment with PEITC are represented in figure 2A. The lowest concentration of 5 µM PEITC caused no significant increase in apoptotic cells after 24 h treatment when compared to the control (ANOVA, $p < 0.83$). However, at concentrations of 10, 20 and 50 µM PEITC, the percentage (mean ± SE) of apoptotic cells at 24 h was 20.5 ± 3.5%, 41.5 ± 6.0% and 79.4 ± 4.3% that was significantly different from controls (ANOVA, $p < 0.01$. In addition, time-dependant effects of 20 and 50 µM PEITC were determined (fig. 2B). The percentage of TUNEL-positive cells increased significantly at 12 and 24 h post-treatment. Consistent with DNA fragmentation were changes in cell size and granularity that were supported by an increase in membrane blebbing and chromatin condensation (data not shown).

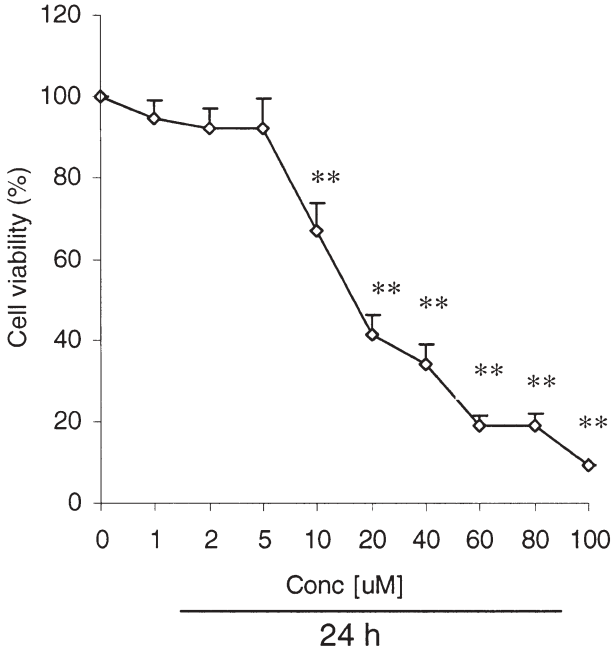

Figure 1. Concentration-dependant changes in cell viability as determined by the MTT assay in HepG2 cells. Cells were treated with 0 (control ± 0.01% DMSO) and PEITC at the concentrations indicated for 24 h. Data are expressed as the mean ± SE of eight or more separate experiments performed on separate days using freshly prepared reagents (** $p < 0.01$).

Figure 2C, D represents the increase in LDH leakage in a concentration- and time-dependant manner in the concentration range 0–50 µM PEITC. The release of LDH into the extracellular medium represents a change in cell membrane viability. After 24 h treatment 10, 20 and 50 µM PEITC showed a significant increase (mean ± SE) in extracellular LDH represented by 15 ± 2.6%, 35 ± 4.7% and 65 ± 6.0% elevation, respectively, compared to the control (ANOVA, $p < 0.01$) (fig. 2C). Lower concentrations of PEITC failed to induce any LDH leakage at any time point. Indeed, LDH leakage observed for 5 µM PEITC was comparable to untreated control cells: 9.43 ± 1.63% and 9.12 ± 1.53%, respectively (ANOVA, $p < 0.8$). PEITC at 20 µM showed no LDH leakage prior to 6 h treatment and extracellular LDH only began to accumulate after 12 h, represented by an increase of 12 ± 1.9%. Indeed, not until 24 h treatment was any significant leakage observed. However, 50 µM PEITC induced a rapid release of LDH at 6 h that was maintained at an elevated level over the time course investigated (50.6 ± 1.9%) (fig. 2D).

Induction of caspase-3 like activity by PEITC in HepG2 cells

Figure 3A, B, represents the concentration- and time-dependant induction of caspase-3-like activity in HepG2 cells mediated by PEITC. The concentration- and time-dependant increases in caspase-3-like activity were determined by measurement of AFC fluorescence intensity derived from the catalytic cleavage of the substrate Ac-DEVD-AFC by endogeneous caspase. The fluorescence intensity of treated over control cells was used to determine the fold increase in caspase activity. In all experiments, 25 ng/ml TNF-α (with 4 µg/ml actinomycin D, 1 h pre-treatment) was used as a positive control typically giving a 3.2 ± 0.3-fold increase after 6 h treatment (mean ± SE).

The time-dependant increase in caspase-3-like activity at a concentration of 20 µM PEITC was observed to be rapid, occurring 1 h after treatment with a 1.45 ± 0.2-fold

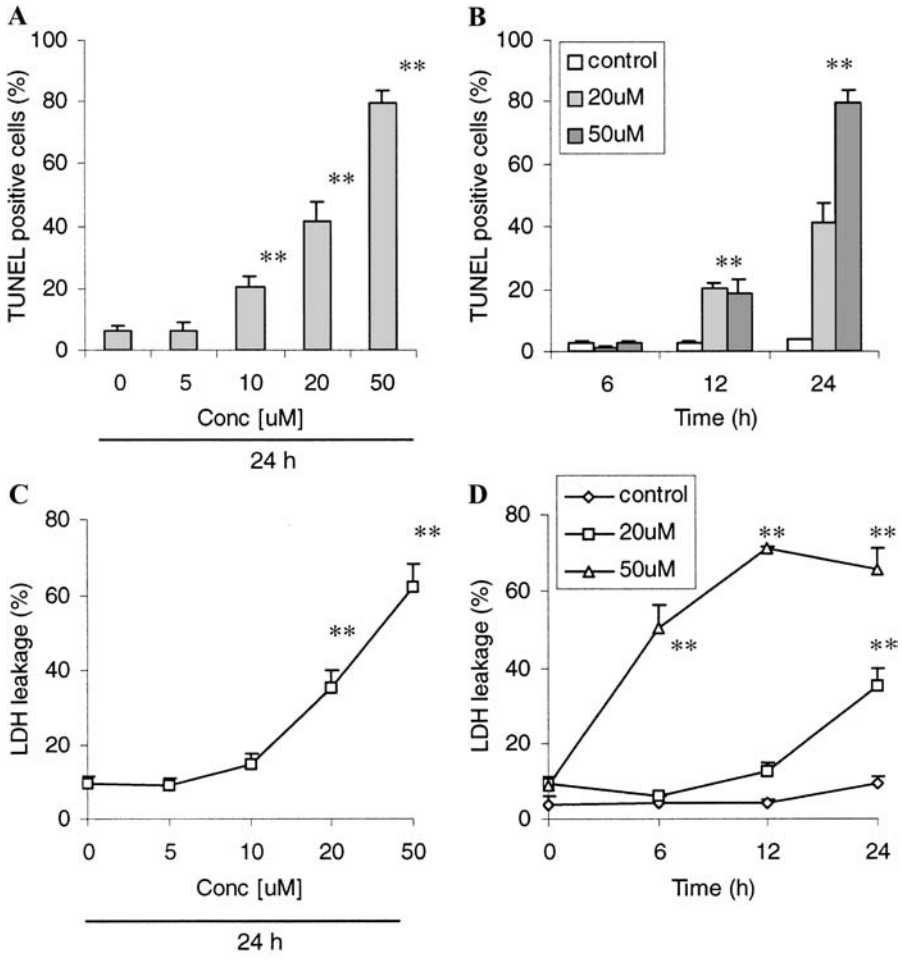

Figure 2. (*A, B*) Concentration at 24 h and time-dependant increases in PEITC-induced apoptosis evaluated by the TUNEL assay. (*C, D*) Concentration at 24 h and time-dependant increases in LDH leakage induced by PEITC in HepG2 cells. Data are expressed as Mean ± SEM of 3 or more separate experiments. (*A–D*) ** Significant difference compared to control (ANOVA, $p < 0.01$).

increase. Prolonged exposure to 20 µM PEITC ultimately led to a 2.48 ± 0.1-fold increase at 12 h that was significantly different from control cells (ANOVA, $p < 0.01$) (fig. 3B). Associated with the rapid induction of caspase-3-like activity was the cleavage of PARP as assessed by Western blot (fig. 3C). The characteristic 116-kDa and associated 85-kDa fragment of PARP were observed in cystolic extracts, treated with PEITC (5–20 µM). The 85-kDa protein appeared as early as 3 h, with maximal PARP cleavage occurring at 12 h. The concentration-dependant increase in PARP cleavage correlated with caspase-3-like activity and DNA fragmentation as determined by the TUNEL assay. At higher concentrations (~50 µM), no caspase-3-like activity or PARP cleavage were observed (fig. 3A, D).

Inhibition of PEITC-induced apoptosis by caspase inhibitors Ac-DEVD-CHO and Z-VAD-FMK

The preliminary data for caspase-3-like activity in HepG2 cells further allowed us to explore the effects of Ac-DEVD-CHO and Z-VAD-FMK on PEITC-induced apoptosis. Pre-treatment (1 h) with either the caspase-3-specific inhibitor Ac-DEVD-CHO (75 µM) or the broad-range caspase inhibitor Z-VAD-FMK (75 µM) significantly reduced caspase-3-like activity (ANOVA, $p < 0.01$) (fig. 4). Associated with the inhibitory effects of both agents was a decrease in the number of TUNEL-positive cells and LDH leakage at 24 h (fig. 4E–G). Typically, 20 µM PEITC induced apoptosis in 41.5 ± 6.0% (mean ± SE) of the cell population as assessed by an increase in TUNEL-positive cells. However, treatment with Z-VAD-FMK significantly inhibited the number of apoptotic cells as observed by a decrease back to control levels, 9.3 ± 3.1%. The reduction in apoptotic cells corresponded to the inhibition of caspase-3-like activity as measured at 12 h (fig. 4F). In contrast, Ac-DEVD-CHO showed only partial protection in PEITC-induced apoptosis, represented by a 50% reduction in TUNEL-positive cells but having a significant inhibitory effect on caspase-3-like activity.

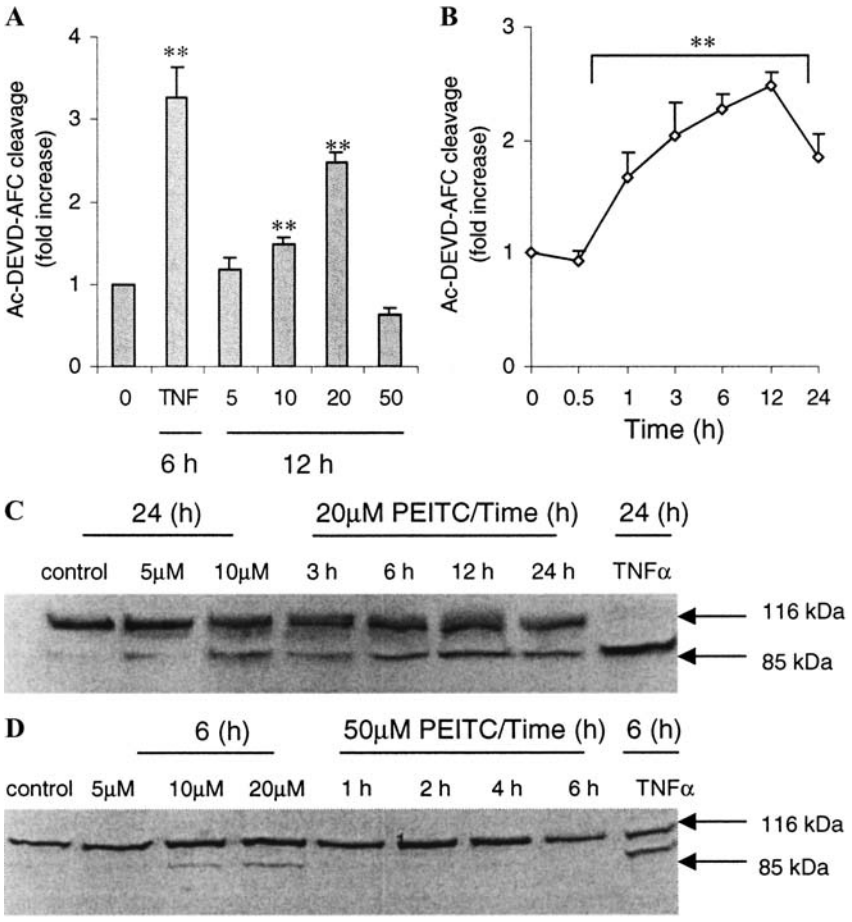

Figure 3. (*A*) Concentration-dependant increase in caspase-3-like activity induced by PEITC measured at 12 h by the increase in fluorescence intensity of liberated AFC from the synthetic substrate Ac-DEVD-AFC. (*B*) Time-dependant increases in caspase-3-like activity 0–24 h (20 μM PEITC). (*A, B*) Data are expressed as the mean ± SE of three or more separate experiments performed on separate days using freshly prepared reagents. (*C*) Concentration- and time-dependant cleavage of PARP induced by PEITC in HepG2 cells. (*D*) Lack of PARP cleavage by 50 μM PEITC over time (0–6 h) is suggestive of necrosis.

PEITC inhibits DNA synthesis and induces G2 M phase cell cycle arrest in HepG2 cells

Analysis of DNA synthesis showed a significant reduction in the incorporation of BrdU in PEITC-treated cells at all concentrations tested. The significant inhibitor effects of 20 μM PEITC were apparent as early as 1 h after treatment with a 35 ± 3.4% reduction in BrdU incorporation when compared with controls (ANOVA, $p < 0.01$). Similar reductions were also observed for 5 and 10 μM PEITC concentrations (fig. 5A, B). We next determined the changes in cell cycle by analysing the distribution of cells within the total population using flow cytometry following PI staining. During the course of exposure to 5–10 μM PEITC, a significant reduction in the number of cells in the G1 phase was observed that corresponded to an increased transition of cells to the G2/M phase (fig. 6A–D). These changes occurred as early as 6 h, peaked at 12 h and subsequently declined at 24 h at 5 μM PEITC, yet were sustained throughout the time course at 10 μM PEITC. Apoptotic concentrations of PEITC (20 μM) had no significant effects on the accumulation of cells in the G2/M phase. Indeed, cell cycle changes were only apparent in the reduction of cells in the G1 phase and this corresponded with a committed increase in the sub-G1 population. Determination of increases in the sub-G1 population within control and treated groups is representative of the formation of mono- and oligo-nucleasomes. One of the major characteristics of apoptosis is the formation of fragmented DNA products. In PEITC-treated cells, sub-G1 populations were observed after 12 h treatment with 20 and 50 μM PEITC. The sub-G1 population reached a maximal increase at 24 h, corresponding with the TUNEL data. Treatments of 5 and 10 μM PEITC showed the formation of a sub-G1 population, however at a lower and less significant incidence (fig 6A).

As lower concentrations of PEITC (5–10 μM) had a significant effect on DNA synthesis and accumulation of cells in the G2/M phase, we next determined changes in

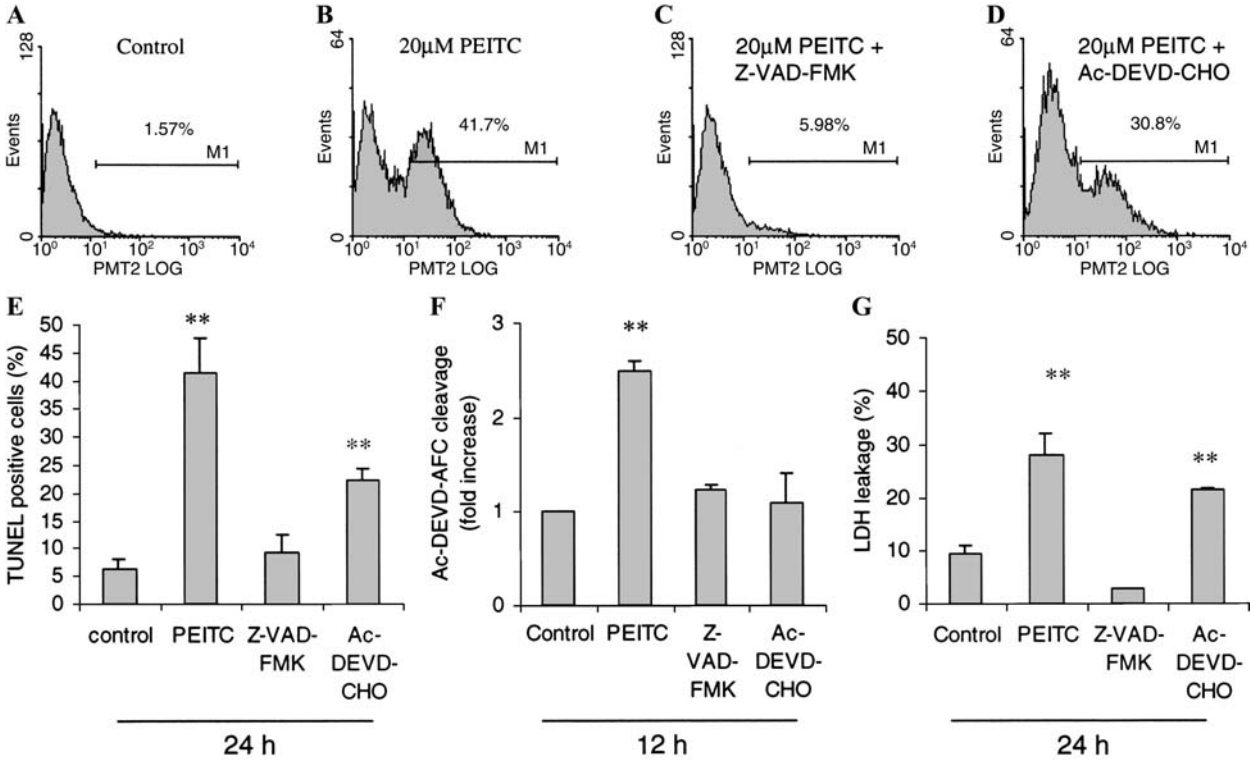

Figure 4. (*A–D*) The inhibitory effects of Z-VAD-FMK and Ac-DEVD-CHO on PEITC-mediated DNA fragmentation in HepG2 cells (*E*) summary of *A–D*. (*F*) Inhibition of caspase-3-like activity by Z-VAD-FMK and Ac-DEVD-CHO in PEITC-treated cells measured at 12 h. (*G*) Associated inhibition of LDH leakage in Z-VAD-FMK- and Ac-DEVD-CHO-treated HepG2 cells. (*E–G*) Data are expressed as mean ± SE of three or more separate experiments performed on separate days using freshly prepared reagents. ** $p < 0.01$.

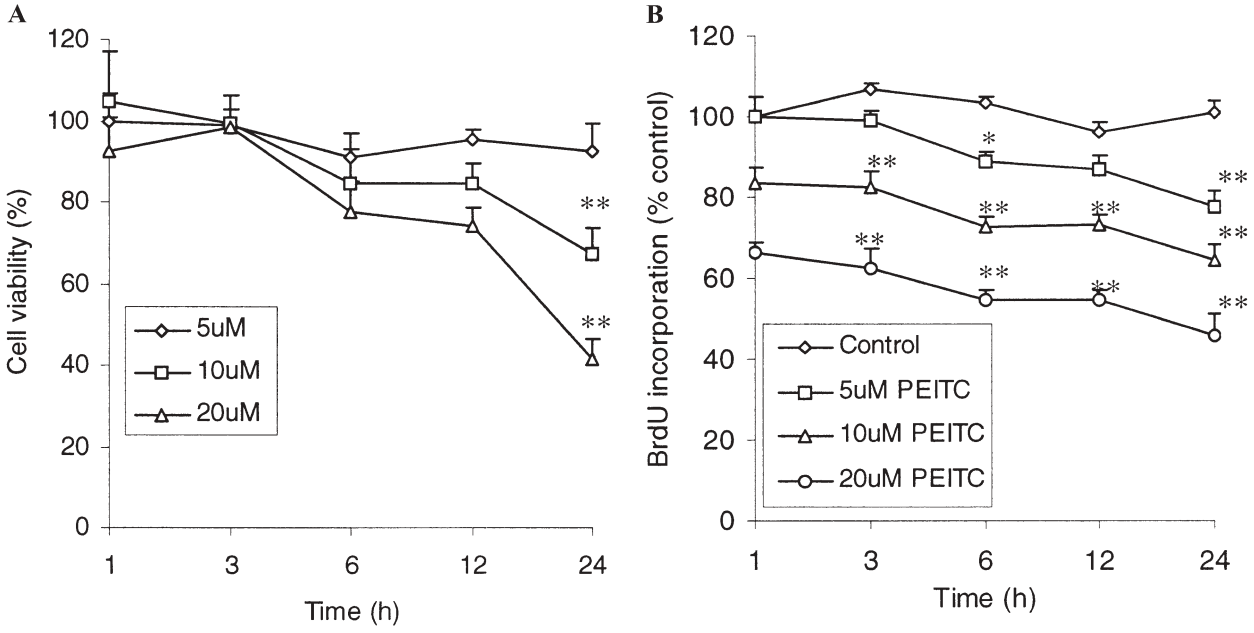

Figure 5. Comparison of cell viability and DNA synthesis in HepG2 cells exposed to PEITC (5–20 μM). Data are expressed as the mean ± SE of three or more separate experiments performed on separate days using freshly prepared reagents. (*A*) Cell viability as determined using the MTT assay following treatment with 5, 10 and 20 μM PEITC at 1–24 h. (*B*) Inhibitory effects of PEITC on DNA synthesis as determined by BrdU incorporation in HepG2 cells.

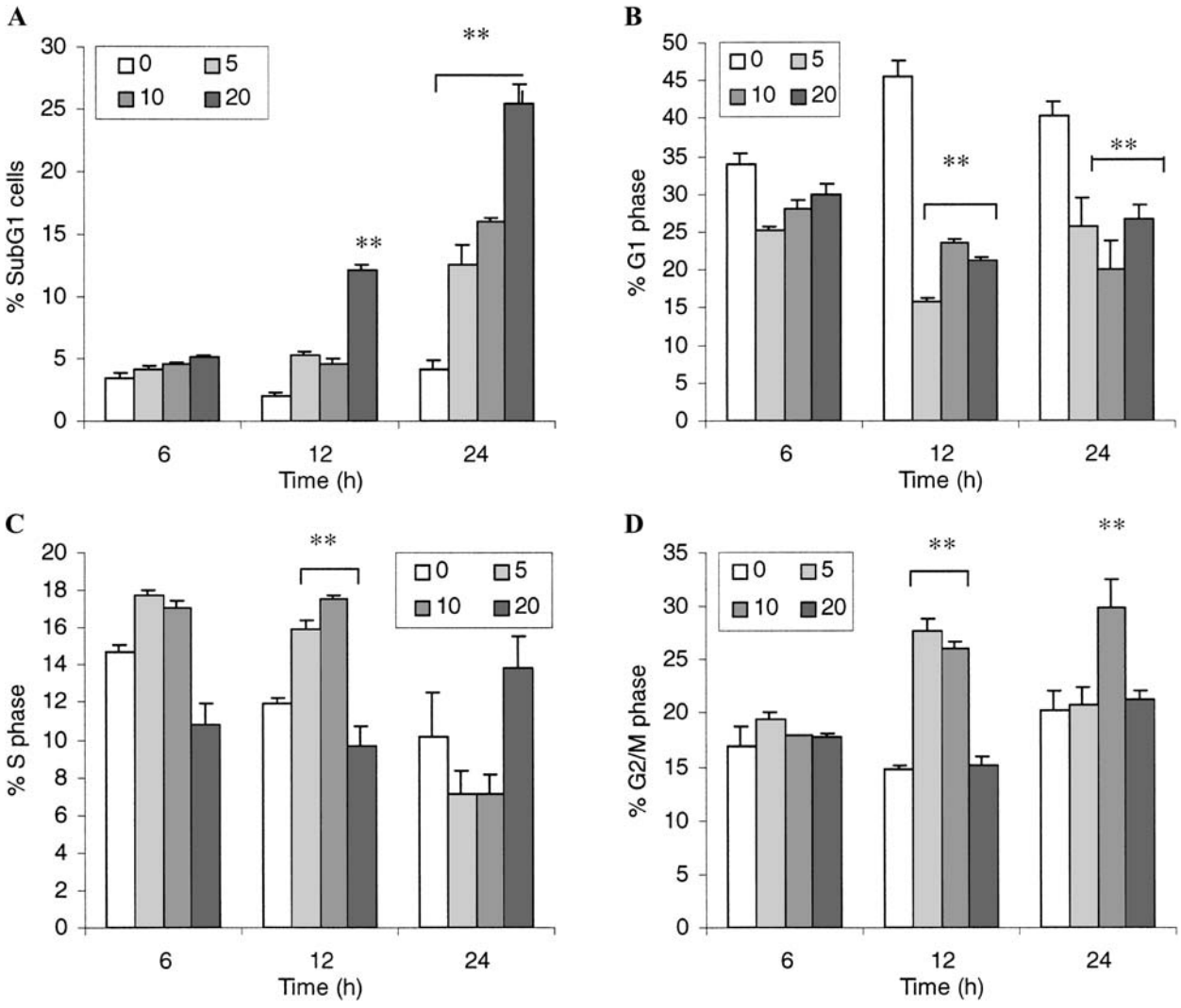

Figure 6. Concentration- and time-dependant effects of PEITC on HepG2 cell cycle distribution measured from 6 to 24 h. Data are expressed as the mean ± SE of three or more separate experiments performed on separate days using freshly prepared reagents (** $p < 0.01$). (*A*) Apoptotic cells (sub-G1 population). (*B*) G1 phase, (*C*) S phase. (*D*) G2/M phase distribution measured from 6 to 24 h.

key cell cycle proteins $p34^{cdc2}$ and cyclin B1. $p34^{cdc2}$ has previously been demonstrated to be a key regulator of the transition through the G2/M phase of the cell cycle [33]. During the onset of G2/M arrest induced by PEITC, we observed a decrease in $p34^{cdc2}$ at both concentrations test (fig. 7A, B). In contrast, cyclin B1 protein levels were increased, this finding being consistent with previous research showing cyclin B1 accumulation in HT29 cells following MSB treatment [12].

PEITC-induced superoxide generation but not hydroperoxides is associated with minor oxidative damage to DNA bases

In our investigations, we observed an early time- and concentration-dependant generation of superoxide ($O_2^{\bullet -}$) in HepG2 cells treated with PEITC that was significantly different from the controls (ANOVA, $p < 0.01$, fig. 8A). Moreover, pre-treatment (1 h) with the SOD mimetic Mn-PyP inhibited $O_2^{\bullet -}$ generation in HepG2 cells exposed to 20 µM PEITC at 3 h as determined by a decrease in DHE fluorescence. In further investigations, we were unable to detect any appreciable levels of peroxide generation by PEITC using carboxy-DCFDA at the same time points (fig. 8B). Using a highly sensitive GC-MS method for the analysis of oxidative DNA base adducts, we next determined the pattern of DNA oxidative damage inducted by PEITC (20 µM). All experiments included a positive control consisting of exposure of HepG2 cells to 1 mM H_2O_2 for 30 min, this leading to the formation of several oxidised adducts derived from both purine and pyrimidine bases that were presumably derived from hydroxyl ($^{\bullet}OH$) radical attack [34, 35]. These included 5-hydroxymethylhydantoin, thymine glycol and 8-hydroxydeoxyguanine and were significantly different from control levels

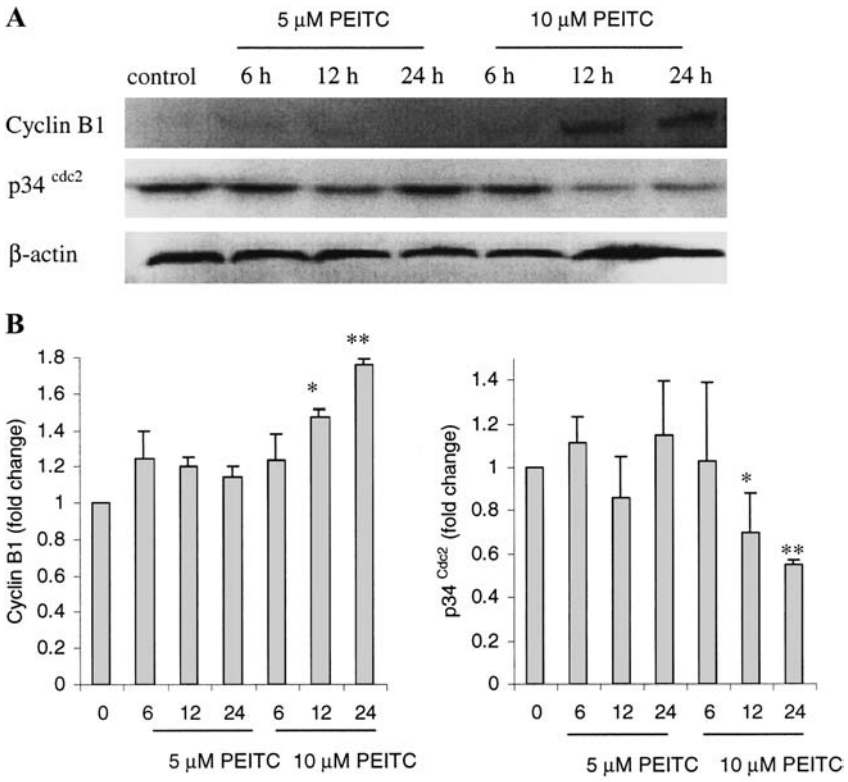

Figure 7. (*A*) Western blot analysis of cyclin B1 and p34^{cdc2} protein changes after treatment with 5–10 μM PEITC for 6, 12 and 24 h. (*B*) Fold changes in cyclin B1 and p34^{cdc2} levels following normalisation to *β*-actin. Data are representative of three separate analyses performed on separate days using freshly prepared samples and reagents. *$p < 0.05$, **$p < 0.01$.

(ANOVA, $p < 0.01–0.04$, fig. 9). Additional base adducts namely 5-formyluracil, FAPy adenine and FAPy guanine were also elevated but to a less significant degree (ANOVA, $p < 0.05$). Likewise, exposure to 20 μM PEITC led to a small increase in thymine glycol, FAPy adenine, FAPy guanine and 8-hydroxyguanine. Although a pattern of oxidative adduct formation was observed in PEITC-treated cells, only minor differences were observed between treated and control cells (ANOVA, $p < 0.3–0.5$).

ROS are not essential for PEITC-induced apoptosis

Based on the findings that 20 μM PEITC could generate an early burst of ROS as measured by superoxide ($O_2^{\bullet -}$) production and promote minor changes in the formation of DNA oxidative base adducts, we next investigated whether pre- and co-treatment with free radical scavengers could prevent or partially protect cells from PEITC-induced apoptosis. This would allow us to determine whether intracellular ROS generation has a primary or secondary role in PEITC-mediated apoptosis. Previous investigations have shown that antioxidants such as Trolox, mannitol, uric acid and ascorbate can diminish intracellular ROS generation induced by apoptotic agents such as arachidonic acid, dopamine and thiolactone [36–38]. The reduction in intracellular ROS production often correlated with the inhibition of or a decrease in the number of apoptotic cells, suggesting intracellular ROS generation plays a role in apoptosis. In our study, neither pre- or co-treatment with non-cytotoxic concentrations (1 mM) of the antioxidants Trolox, ascorbate, mannitol and uric acid had any appreciable inhibitory effects on PEITC- (20 μM) induced apoptosis as determined by the MTT or crystal violet assay at 24 h (fig. 10). In addition, the superoxide mimetic MnPyP (50 μM) that has previously been shown to inhibit both CYP2E1 toxicity and neural and peroxynitrite-induced apoptosis as well as hydrogen peroxide-induced DNA strand breakage had no inhibitory effects [39–42]. These data suggest that ROS generation is likely to be a secondary effect of PEITC-mediated apoptosis.

Discussion

The chemopreventative properties of dietary-derived ITCs have been extensively studied in vivo and in vitro [1, 43–45]. One of the most promising is PEITC, a major constituent of the salad crops watercress, *R. nasturtium aquaticum* and landcress *Barbarea vulgaris*. Among its many properties, PEITC is able to induce phase II detox-

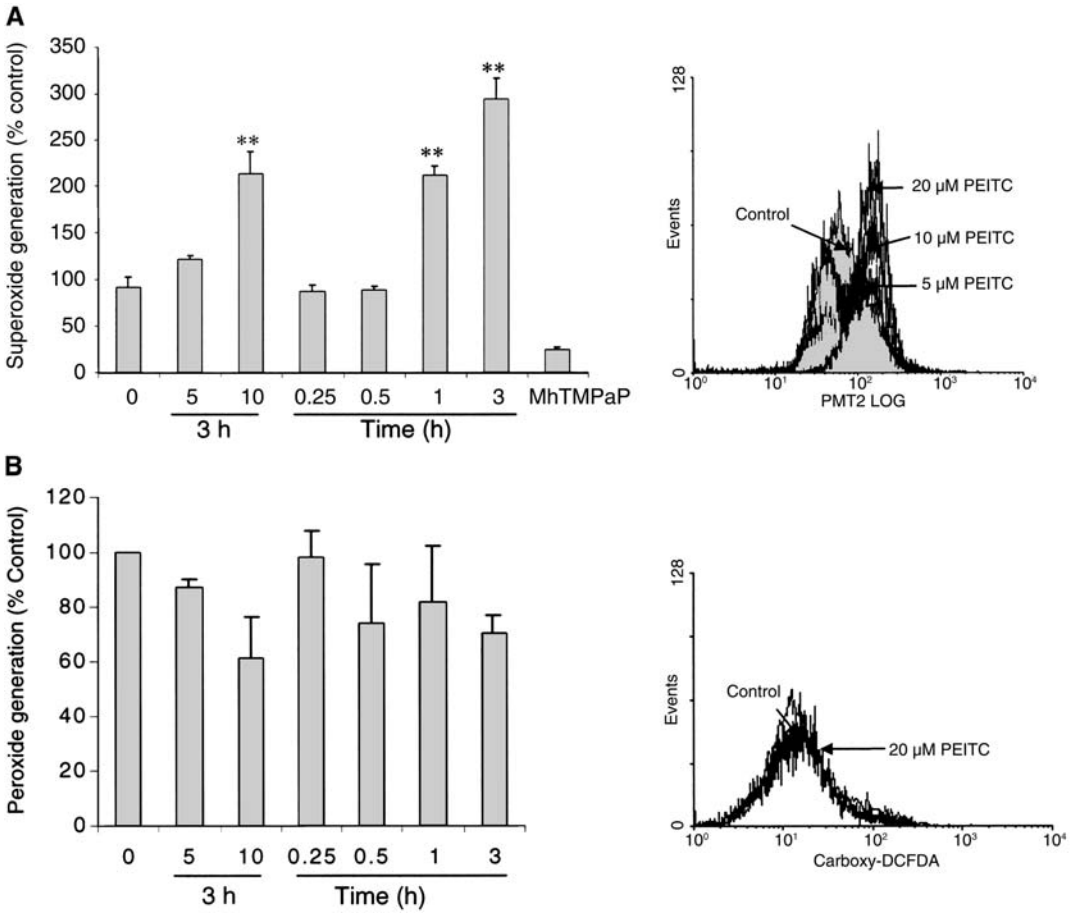

Figure 8. (*A*) Time- and concentration-dependant generation of superoxide induced by 20 μM PEITC in HepG2 cells and inhibition of PEITC-mediated ROS generation by the SOD mimetic MnPyP (50 μM). (*B*) Lack of detectable hydroperoxide generation by PEITC using carboxy-DCFDA. (*A, B*) Data are representative of three separate experiments (mean ± SD) performed on separate days using freshly prepared samples and reagents.

ification enzymes, a function shown to aid carcinogen excretion. However, recent reports have also implicated PEITC as a potent inducer of apoptosis. In the present paper, we demonstrated that PEITC induces concentration- and time-dependant increases in apoptosis in human hepatoma HepG2 cells. Apoptosis was characterised by a committed increase in caspase-3-like activity and associated cleavage of PARP. Treatment with the broad-range caspase inhibitor Z-VAD-FMK inhibited caspase-3-like activity and prevented apoptosis, these findings corresponding with previous reports [15, 17]. The partial inhibitory effect of Ac-DEVD-CHO on the number of apoptotic cells, although inhibiting caspase-3-like activity, suggests that other proteolytic enzymes are involved in PEITC-induced apoptosis. Indeed, both caspase-8 and caspase-9 have been implicated in ITC-induced apoptosis [17, 24]. The final terminal event of apoptosis is the committed increase in DNA fragmentation and loss of membrane viability. In this study, apoptosis was assessed by analysis of TUNEL and sub-G1 formation and the results corresponded well with caspase activity and PARP cleavage. Furthermore, the onset of DNA fragmentation that occurred as early as 12 h corresponded with a concentration- and time-dependant increase in changes in cell morphology and LDH leakage (fig. 2).

Further to the ability of PEITC to induce apoptosis, we also demonstrated that high concentrations were capable of inducing necrosis. At 50 μM PEITC, no caspase-3-like activity or PARP cleavage were observed even though DNA fragmentation was detected. These data correspond with findings that 50 μM benzyl ITC (BITC) caused a reduction in caspase-3-like activity in rat liver epithelial RL34 cells [24]. Moreover, other cytotoxic agents have been shown to impair caspase-3-like activity and PARP cleavage, while additional research has shown that the TUNEL assay is incapable of discriminating between necrosis and apoptosis [46–48]. These characteristics were all observed at 50 μM PEITC treatments in HepG2 cells and are suggestive of necrosis.

In addition to the induction of apoptosis, we also demonstrated the ability of PEITC to block cells in the G2/M phase of the cell cycle. The transient accumulation of

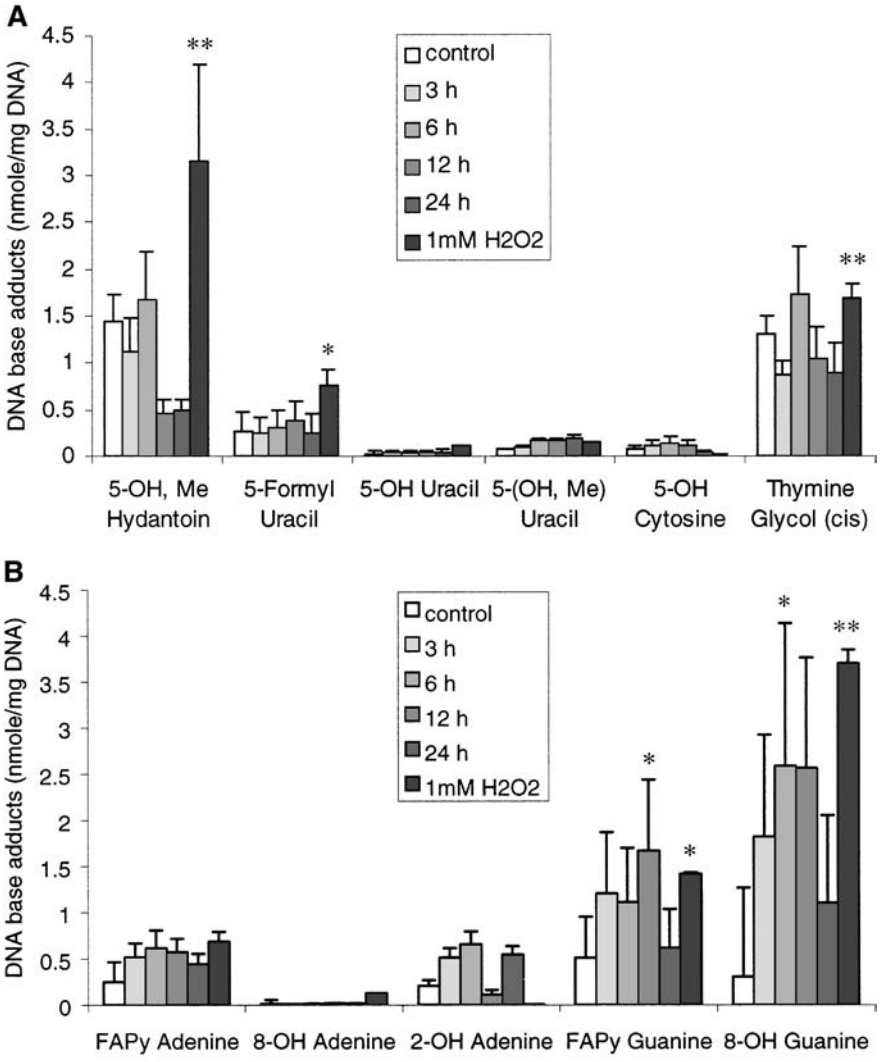

Figure 9. GC-MS analysis of oxidative DNA base adducts derived from HepG2 cells following exposure to an apoptotic concentration of PEITC (20 μM) measured from 3 to 24 h, in addition to treatment with 1 mM H_2O_2 for 30 min as a positive control. Data are representative of at least three separate experiments (mean ± SD) performed on separate days using freshly prepared samples and reagents. * $p < 0.05$, ** $p < 0.01$.

cells in the G2/M population correlated with an increase in cyclin B1 and a reduction in $p34^{cdc-2}$ protein. Inhibition of $p34^{cdc-2}$ kinase activity has previously been shown to lead to a cell block in the G2/M phase [49–50]. Likewise, an increase in cyclin B1 protein levels has previously been associated with G2/M phase arrest [12]. This mechanism may serve as an alternative means by which PEITC offers chemoprotective effects, by allowing cells to repair damaged DNA before re-entry into the cell cycle.

We next addressed whether PEITC could induce the generation of intracellular ROS and whether this had any function in PEITC-mediated apoptosis. Preliminary studies using DHE to measure $O_2^{\bullet-}$ generation revealed a time- and concentration-dependant increase in $O_2^{\bullet-}$ in HepG2 exposed to PEITC. No such increases were observed for peroxide generation using carboxy-DCFDA. To circumvent these anomalies, we used a highly sensitive, quantitative GC-MS method to determine the occurrence of oxidative DNA base biomarkers in HepG2 cells following exposure to 20 μM PEITC. This has the advantage over HPLC techniques since it allows the measurement of several DNA base oxidation products simultaneously using heavy isotope internal standards. We were therefore able to determination a 'fingerprint' of causative ROS damage by PEITC in our system. For example, GC-MS methodologies have been used to show hydroxyl radical ($^{\bullet}OH$) attack of all four bases resulting in multiple products, whereas singlet oxygen only attacks guanine [34]. Reactive nitrogen species such as peroxynitrite ($ONOO^-$) and reactive chlorine species such as hypochlorous acid (HOCl) attack purine [35] and pyrimidine bases [32], respectively. All experiments included

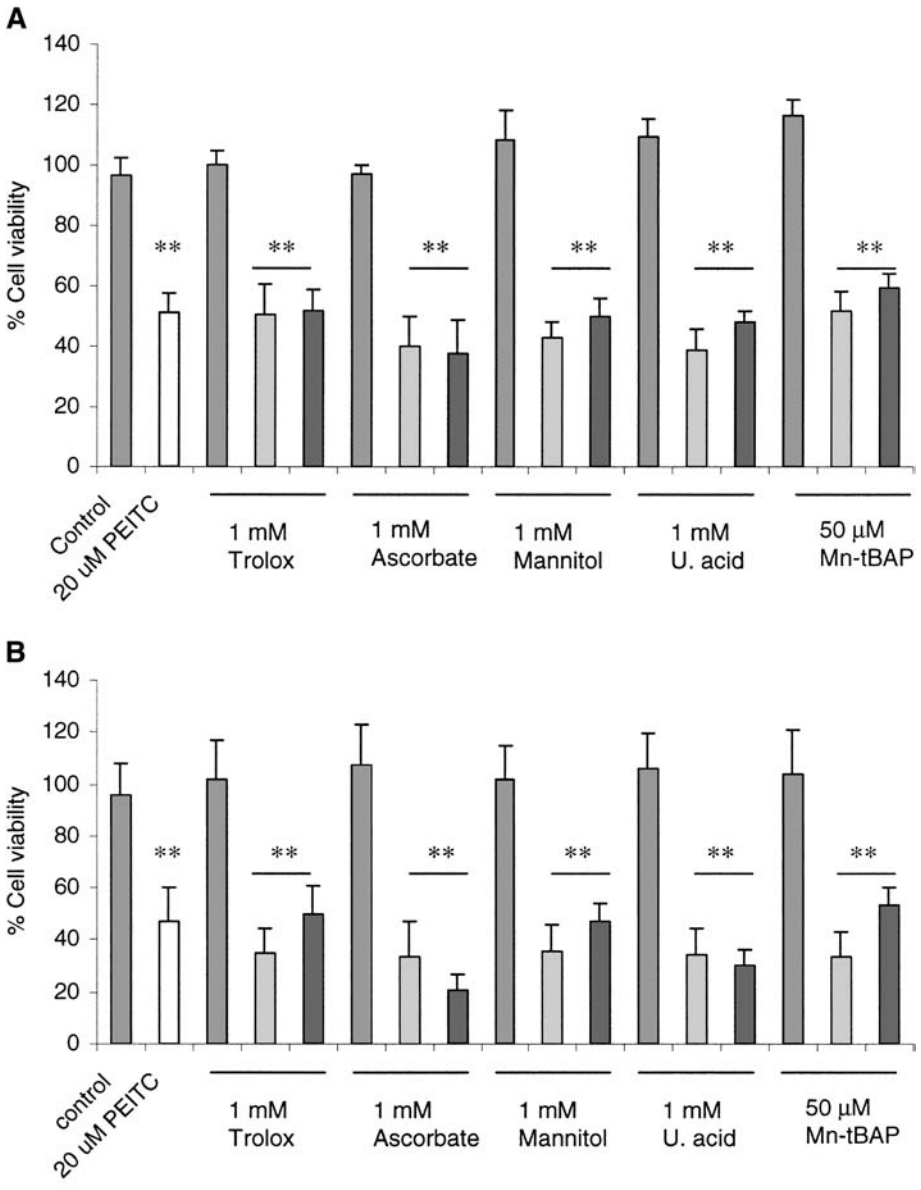

Figure 10. Lack of inhibition by antioxidants of PEITC-mediated apoptosis in HepG2 cells. Crystal violet assay (*A*) and MTT test for cell viability (*B*). Cells were pre- (light-grey bars) and co-treated (dark-grey bars) with a non-toxic concentration (1 mM) of Trolox, ascorbate, mannitol and uric acid or 50 µM MnPyP of the SOD mimetic for 1 h before exposure to 20 µM PEITC for 24 h. Data are representative of at least eight separate experiments (mean ± SD) performed on three separate occasions (ANOVA, ** $p < 0.01$).

DNA samples obtained from exposing HepG2 cells to 1 mM hydrogen peroxide (H_2O_2) for 30 min, and served as a positive control for DNA base adduct formation. Although no significant changes were observed between treated and control groups in PEITC-treated cells, a visible time-dependant increase in some adducts was apparent. These bases have previously been identified as being susceptible to hydroxyl radical attack in epithelial cells exposed to hydrogen peroxide [50]. Previous investigations have shown an increase in the oxidative DNA biomarker 8-OHdG in HL60 cells exposed to allyl ITC, as well as an increase in cellular lipid peroxidation induced by BITC in vitro [51, 52]. To determine whether ROS was the primary cause of apoptosis induced by PEITC, we examined the effects of antioxidant treatments on PEITC-mediated apoptosis. Using Trolox and ascorbate, both effective ROS scavengers, mannitol, a hydroxyl radical ($^{\bullet}OH$) scavenger, uric acid, a potent peroxynitrite ($ONOO^-$) scavenger and the superoxide ($O_2^{\bullet -}$) radical scavenger MnPyP, we found no protective effects as measured by the MTT and crystal violet assays. In addition, co-treatment with superoxide dismutase (250 U/ml) and catalase (400 U/ml) failed to prevent PEITC-induced apoptosis (data not shown). Our investigations are thus

suggestive that although intracellular ROS levels are increased after PEITC treatment, they are probably a secondary effect and not involved in the apoptotic cascade. However, we do believe that future work is still required to determine the origins of ITC-induced ROS production. Current data suggest that ITCs are effective uncouplers of the mitochondria respiratory chain [53] with additional investigations showing that superoxide ($O_2^{\bullet -}$) production originates from the mitochondrial respiratory complexes [54]. Indeed, Dussman et al. [55] observed an increased production of superoxide ($O_2^{\bullet -}$) by mitochondria in cells undergoing apoptosis. Moreover, the increase in superoxide ($O_2^{\bullet -}$) was associated with the release of intermembrane proteins such as cytochrome C. Mitochondrial cytochrome C release has previously being observed in MSB-induced apoptosis in HT29 cells [12]. In addition, future investigations should determine whether other oxidative biomarkers are more suitable for studying ITC-induced ROS, and determine whether changes in other cellular parameters such as glutathione depletion and/or an increase in intracellular iron or copper content can potentate ROS generation, leading to an increase in cellular toxicity.

In summary, we demonstrated that PEITC is effective in inducing apoptosis in mammalian cancer cells. Our data along with those of several other groups suggest that ITC-induced apoptosis in vitro involves a common apoptotic pathway with caspase-3 being a common element in the apoptotic cascade. We also showed that PEITC is effective in inducing G2/M phase cell cycle arrest, a phenomenon associated with an increase in cyclin B1 and a reduction in $p34^{cdc2}$ proteins.

Consumption of 30 g fresh weight of watercress is estimated to expose an individual to approximately 21.6 mg of β-phenylethyl glucosinolate, or alternatively, 7.6 mg of PEITC, approximately 50% of which is excreted in the urine as the respective mercapturic acid metabolite [56]. Previous work has also demonstrated that the intracellular levels of ITCs in murine hepa 1c1c7 cells can attain millimolar concentrations [57]. This would suggest that apoptotic-inducing concentrations are attainable in vivo. These data imply that apoptosis may play a significant role in PEITC chemoprevention. Also demonstrated was the ability of PEITC to circumvent the caspase-mediated apoptotic pathway switching programmed cell death to necrosis. These data highlight the deleterious effects that may be attained from excessive amounts of PEITC. Indeed, this may partially explain the gross morphological changes in liver after exposure to PEITC [58]. Moreover, we have demonstrated for the first time a committed generation of superoxide ($O_2^{\bullet -}$) that correlates with minor changes in the levels of oxidative DNA base adducts in PEITC-treated cells. The increase in intracellular ROS appears to be a secondary effect of PEITC exposure and is likely to originate from subcellular organelles rather than being generated in the extracellular media, as has previously been found for many of the polyphenolics [59]. Intracellular ROS may feasibly play a role in enzyme induction and or stress signalling that are characteristics of ITC exposure. These are currently under investigation in our laboratory. Taken together, our data demonstrate the potential of PEITC as a chemoprotective agent; however, further work is required to elucidate the apoptotic cascade and the role it plays in ITC chemoprevention and/or toxicity.

Acknowledgements. The authors would like to thank Dr W. X. Ding and Ms B. L. Ng for their technical support in flow cytometry.

1 Block G., Patterson B. and Subar A. (1992) Fruit, vegetables and cancer prevention: a review of the epidemiological evidence. Nutr. Cancer **1:** 1–29
2 Verhoeven D. T., Verhagen H., Goldbohm R. A. and Van Poppel G. (1997) A review of the mechanisms underlying anticarcinogenicity by brassica vegetables. Chem. Biol. Interact. **103:** 79–129
3 Rask L., Andreasson E., Ekbom B., Eriksson S., Pontoppidan B. and Meijer J. (2000) Myrosinase: gene family evolution and herbivore defence in Brassicaceae. Plant. Mol. Biol. **42:** 93–113
4 Fahey J. W., Zalcmann A. T. and Talalay P. (2001) The chemical diversity and distribution of glucosinolates and isothiocyanates among plants. Phytochemistry **56:** 5–51
5 Zhang Y. and Talalay P. (1994) Anticarcinogenic activities of organic isothiocyanates: chemistry and mechanisms. Cancer Res. **54:** 1976s–1981s.
6 Zhang Y. and Talalay P. (1998) Mechansim of differential potencies of isothiocyanates as inducers of anticarcinogenic phase 2 enzymes. Cancer Res. **58:** 4632–4639
7 Rose P., Faulkner K., Williamson G. and Mithen R. (2000) 7-Methylsulphinylheptyl and 8-methylsulphinyloctyl isothiocyanates from watercress are potent inducers of phase II enzymes. Carcinogenesis **21:** 1983–1988
8 Hecht S. S., Carmella S. G. and Murphy S. E. (1999) Effects of watercress on urinary metabolites of nicotine in smokers. Cancer Epidemiol. Biomarkers Prev. **8:** 907–913
9 London S. J., Yuan J. M., Chung F. L., Gao Y. T., Coetzee G. A., Ross R. K. et al. (2000) Isothiocyanates, glutathione-S-transferase M1 and T1 polymorphisms, and lung cancer risk: a prospective study of men in Shanghai, China. Lancet **356:** 724–729
10 Zhao B., Seow A., Lee E. J., Poh W. T., The M., Eng P. et al. (2001) Dietary isothiocyanates, glutathione-S-transferase-M1, -T1 polymorphisms and lung cancer risk among Chinese women in Singapore. Cancer Epidemiol. Biomarkers Prev. **10:** 1063–1067
11 Lin H. J., Probst-Hensch N. M., Louie A. D., Kau I. H., Witte J. S., Ingles S. et al. (1998) Glutathione transferase null genotype, broccoli, and lower prevalence of colorectal cancer. Cancer Epidemiol. Biomarkers Prev. **8:** 647–652
12 Gamet-Payrastre L., Li P., Lumeau S., Cassar G., Dupont M. A., Chevolleau S. et al. (2000) Sulforaphane, a naturally occurring isothiocyanate, induces cell cycle arrest and apoptosis in HT29 human colon cancer cells. Cancer Res. **60:** 1426–1433
13 Chiao J. W., Chung F. L, Kancherla R., Ahmed T., Mittelman A. and Conaway C. C. (2002) Sulforaphane and its metabolite mediate growth arrest and apoptosis in human prostate cancer cells. Int. J. Oncol. **20:** 631–636
14 Chen Y.-R., Wang W., Kong A. N. and Tan T.-H. (1998). Molecular mechanisms of c-jun N-terminal kinase-mediated apopto-

sis induced by anticarcinogenic isothiocyanates. J. Biol. Chem. **273:** 1769–1775
15 Haung C., Ma W. Y., Li J., Hecht S. S. and Dong Z. (1998) Essential role of p53 in phenylethyl isothiocyanate induced apoptosis. Cancer Res. **58:** 4102–4106
16 Xiao D. and Singh S. V. (2002) Phenylethyl isothiocyanate induced apoptosis in p53 deficient PC 3 human prostate cancer cell line is mediated by extracellular signal regulated kinase. Cancer Res. **62:** 3615–3619
17 Xu K. and Thornalley P. J. (2000) Studies on the mechanism of the inhibition of human leukemia cell growth by dietary isothiocyanates and their cysteine adducts in vitro. Biochem. Pharmacol. **60:** 221–231
18 Xu K. and Thornalley P. J. (2001) Signal transduction activated by cancer chemopreventive isothiocyanates: cleavage of BID protein, tyrosine phosphorylation and activation of JNK. Br. J. Cancer. **84:** 670–673
19 Yang Y. M., Conaway C. C., Chiao J. W., Wang C. X., Amin S., Whysner J. et al. (2002) Inhibition of benzo[a]pyrene induced lung tumorigenesis in A/J mice by dietary N-acetylcysteine conjugates of benzyl and phenylethyl isothiocyanates during the postinitiation phase is associated with the activation of mitogen activated protein kinases and p53 activity and induction of apoptosis. Cancer Res. **62:** 2–7
20 Kulms D., Zeise E., Poppelmann B. and Schwarz T. (2002) DNA damage, death receptor activation and reactive oxygen species contribute to ultraviolet radiation-induced apoptosis in an essential and independent way. Oncogene. **21:** 5844–5851
21 Moreno-Manzano V., Ishikawa Y., Lucio-Cazana J. and Kitamura M. (2000) Selective involvement of superoxide anion, but not downstream compounds hydrogen peroxide and peroxynitrite in tumor necrosis factor alpha induced apoptosis in rat mesangial cells. J. Biol. Chem. **275:** 12684–12691
22 Groninger E., Meeuwsen-De Boer G. J., De Graaf S. S., Kamps W. A. and DeBont E. S. (2002) Vincristine induced apoptosis in acute lymphoblastic leukaemia cells: a mitochondrial controlled pathway regulated by reactive oxygen species? Int. J. Oncol. **21:** 1339–1345
23 Luo J., Sun Y., Lin H., Qian Y., Li Z., Leonard S. S. et al. (2003) Activation of c-jun NH2-terminal kinase (JNK) by vanadate induces FADD-dependant death of cerebellar granule progenitors in vitro. J. Biol. Chem. **278:** 4542–4551
24 Nakamura Y., Kawakami M., Yoshihiro A., Miyoshi N., Ohigashi H., Kawai K. et al. (2002) Involvement of the mitochondrial death pathway in chemopreventive benzyl isothiocyanate induced apoptosis. J. Biol. Chem. **277:** 8492–8499
25 Nicoletti I., Migliorati G., Pagliacci M. C., Grignani F. and Riccardi C. (1991) A rapid and simple method for measuring thymocyte apoptosis by propidium iodide staining and flow cytometry. J. Immunol. Methods **139:** 271–279
26 Shen H. M., Yang C. F. and Ong C. N. (1999) Sodium selenite induced oxidative stress and apoptosis in human HepG2 cells. Int. J. Cancer. **81:** 820–828
27 Hansen M. B., Nielsen S. E. and Berg K. (1989) Re-examination and further development of a precise and rapid dye method for measuring cell growth/cell kill. J. Immunol. Methods. **119:** 203–210
28 LeBel C. P., Ischiopoulos H. and Bondy S. C. (1992) Evaluation of the probe 2′,7′-dichlorofluorescin as indicator of reactive oxygen species formation and oxidative stress. Chem. Res. Toxicol. **5:** 227–231
29 Roche G. and Valet G. (1990) Flow cytometry analysis of respiratory burst activity in phagocytes with hydroethidine and 2′,7′ dichlorofluorescein. J. Leukoc. Biol. **47:** 440–448
30 Jenner A., England T. G., Aruoma O. I. and Halliwell B. (1998) Measurement of oxidative DNA damage by gas chromatography-mass spectrometry: ethanethiol prevents artifactual generation of oxidized DNA bases. Biochem. J. **331:** 365–369
31 England T. G., Jenner A., Aruoma O. I. and Halliwell B. (1998) Detection of oxidative DNA base damage by gas chromatography-mass spectrometry: effects of derivatization conditions on artifactual formation of certain base oxidation products. Free. Radic. Res. **29:** 321–330
32 Whiteman M., Hong S. H., Jenner A. and Halliwell B. (2002) Loss of oxidized and chlorinated bases in DNA treated with reactive oxygen species: implications for assessment of oxidative damage in vivo. Biochem. Biophys. Res. Commun. **296:** 883–889
33 King R. W. and Jackson P. K. (1994) Mitosis in transition. Cell **79:** 563–571
34 Halliwell B. and Gutteridge J. M. C. (1999) Free Radicals in Biology and Medicine, 3rd edn, Clarendon, Oxford
35 Spencer J. P., Jenner A., Chimel K., Aruoma O. I., Cross C. E., Wu R. et al. (1996) DNA strand breakage and base modification induced by hydrogen peroxide of human respiratory tract epithelial cells. FEBS. Lett. **374:** 233–236
36 Wu D. and Cederbaum A. I. (2002) Cyclosporin A protects against arachidonic acid toxicity in rat hepatocytes: role of CYP2E1 and mitochondria. Hepatology **35:** 1420–1430
37 Jones D. C., Gunasekar P. G., Borowitz J. L. and Isom G. E. (2000) Dopamine induced apoptosis is mediated by oxidative stress and is enhanced by cyanide in differentiated PC12 cells. J. Neurochem. **74:** 2296–2304
38 Huang R. F., Huang S. M., Lin B. S., Hung C. Y. and Lu H. T. (2002) N-acetylcysteine, vitamin C and vitamin E diminish homocysteine thiolactone induced apoptosis in human promyeloid HL-60 cells. J. Nutr. **132:** 2151–2156
39 Patel M. (1998) Inhibition of neural apoptosis by a metalloporphyrin superoxide dismutase mimic. J. Neurochem. **71:** 1068–1074
40 Choi I. Y., Lee S. J., Ju C., Nam W., Kim H. C., Ko K. H. et al. (2000) Protection by a manganese porphyrin of endogeneous peroxynitrite induced death in glial cells via inhibition of mitochondrial transmembrane potential decrease. Glia. **31:** 155–164
41 Szabo C., Day B. J. and Salzman A. L. (1996) Evaluation of the relative contribution of nitric oxide and peroxynitrite to the suppression of mitochondrial respiration in immunohistostimulated macrophages using a manganese mesoporphyrin superoxide dismutase mimetic and peroxynitrite scavenger. FEBS. Lett. **381:** 82–86
42 Perez M. J. and Cederbaum A. I. (2002) Antioxidant and prooxidant effects of a manganese porphyrin complex against CYP2E1 toxicity. Free. Radic. Biol. Med. **33:** 111–127
43 Chung F. L., Kelloff G., Steele V., Pittman B., Zang E., Jiao D. et al. (1996) Chemopreventive efficacy of aryalkyl isothiocyanates and N-acetylcysteine for lung tumorigenesis in Fischer rats. Cancer Res. **56:** 772–778
44 Chung F. L., Conaway C. C., Rao C. V. and Reddy B. S. (2000) Chemoprevention of colonic aberrant crypt foci in Fischer rats by sulforaphane and phenylethyl isothiocyanate. Carcinogenesis **21:** 2287–2291
45 Conaway C. C., Jiao D. and Chung F. L. (1996) Inhibition of rat liver cytochrome P450 isoenzymes by isothiocyanates and their conjugates: a structure activity relationship study. Carcinogenesis **17:** 2423–2427
46 Higuchi Y. and Yoshimoto T. (2002) Arachidonic acid converts the glutahtione depletion induced apoptosis to necrosis by promoting lipid peroxidation and reducing caspase 3 activity in rat glioma cells. Arch. Biochem. Biophys. **400:** 133–140
47 Lopez-Marure R., Gutierrez G., Mendoza C., Ventura J. L., Sanchez L., Reyes Maldonado E. et al. (2002) Ceramide promotes the death of human cervical tumor cells in the absence of biochemical and morphological markers. Biochem. Biophys. Res. Commun. **293:** 1028–1036
48 Grasl-Kraupp B., Ruttkay-Nedecky B., Koudelka H., Bukowska K., Bursch W. and Schulte-Hermann R. (1995) In situ detection

of fragmented DNA (TUNEL assay) fails to discriminate among apoptosis, necrosis and autolytic cell death: a cautionary note. Hepatology **21:** 1465–1468

49 Aytac U., Claret F. X., Kazuya S., Ohnuma K., Mills G. B., Cabanillas F. et al. (2001) Expression of CD26 and its associated dipeptidyl peptidase IV enzyme activity enhances sensitivity to doxorubicin induced cell cycle arrest at the G2/M checkpoint. Cancer Res. **61:** 7204–7210

50 Tyagi A. K., Singh P. R., Agarwal C., Chan D. C. F. and Agarwal R. (2002) Silibinin strongly synergizes human prostate carcinoma DU145 cells to doxorubicin induced growth inhibition, G2/M arrest and apoptosis. Clin. Cancer Res. **8:** 3512–3519

51 Murata M., Yamashita N., Inoue S. and Kawanishi S. (2000) Mechanism of oxidative DNA damage induced by carcinogenic allyl isothiocyanate. Free Radic. Biol. Med. **28:** 797–805

52 Kassie F., Pool-Zobel B., Parzefall W. and Knasmuller S. (1999) Genotoxic effects of benzyl isothiocyanate, a natural chemopreventive agent. Mutagenesis **14:** 595–604

53 Miko M. and Chance B. (1975) Isothiocyanates: a new class of uncouplers. Biochim. Biophys. Acta **396:** 165–174

54 Li N., Ragheb K. E., Lawler G., Sturgis J., Rajwa B., Melendez J. A. and Robinson J. P. (2002) Mitochondrial complex I inhibitor rotenone induces apoptosis through enhancing mitochondrial reactive oxygen species production. J. Biol. Chem. **278:** 8516–8525

55 Dussmann M., Kogel D., Rehm M. and Prehn J. H. (2003) Mitochondrial membrane permeabilization and superoxide production during apoptosis: a single-cell analysis. J. Biol. Chem. **278:** 12645–12649

56 Chung F.-L., Morse M. A., Eklind K. L. and Lewis J. (1992) Quantitation of human uptake of the anticarcinogen phenylethyl isothiocyanate after a watercress meal. Cancer Epidemiol. Biomarkers Prev. **1:** 383–388

57 Zhang Y. (2000) Role of glutathione in the accumulation of anticarcinogenic isothiocyanates and their glutathione conjugates by murine hepatoma cells. Carcinogenesis **21:** 1175–1182

58 Gray R. H., Adam-Rodwell G. A., Maris D., Haskins J. R. and Stoner G. D (1995) Quantitative microscopy of hepatic changes induced by β-phenethyl isothiocyanate in Fischer-344 rats fed either a cereal based diet or a purified diet. Toxicol. Pathol. **23:** 644–652

59 Long L. H., Clement M. V. and Halliwell B. (2002) Artifacts in cell culture: rapid generation of hydrogen peroxide on addition of (–)epigallocatechin, (–)epigallocatechin gallate, (+)catechin and quercetin to commonly used cell culture media. Biochem. Biophys. Res. Commun. **273:** 50–53